Treatment of Cloud Radiative Effects in General Circulation Models

W.-C. Wang, X.-Z. Liang, M. Ding, E. Joseph and L. Zhu
Atmospheric Sciences Research Center
State University of New York
Albany, New York

Summary

We participate in the Atmospheric Radiation Measurement (ARM) Program with two objectives: 1) to improve general circulation model (GCM) treatment of the subgrid-scale variability of cloud-radiation interaction and 2) to study the effect of the variability on GCM climate simulations. This report summarizes recent project findings, with focus on the further development of the "mosiac" approach to treat the subgrid-scale variability of cloud-radiation interaction. The progress on radiative effects of cirrus clouds is briefly discussed.

Parameterization for Subgrid-Scale Cloud-Radiation Interaction

The "Mosaic" Approach

Current GCMs simulate only cloud fractions in individual model layers without explicitly specifying their association. However, there exists a strong vertical geometric association for convective (Cc), anvil cirrus (Ci), and stratiform (Cs) clouds (see Figure 1). Because the distribution of radiative heating/cooling is sensitive to cloud cover, it is quite clear that proper consideration of the inherent geometric association of the clouds is needed. Using ARM data and simulations from a regional climate model over the Southern Great Plains (SGP) site (Dudek et al. 1996), we have developed a "mosaic" approach to parameterize the subgrid-scale variability associated with cloud macrogrouping and inhomogeneity (Liang and Wang 1997).

In the "mosaic" treatment, the GCM grid is divided into subcells filled horizontally by a specific cloud genus (or sometimes two cloud genera) with distinct optical properties. Different cloud genera (Cc, Ci, Cs) in each layer are first defined to be geographically distinct and thus minimally overlapped. Second, Cc are assigned to a single subcell, where the area is given by the largest Cc values from the convective top to the lowest layers. Third, Ci (usually in the convection top layer) then fill consecutively the subcells that are equally divided over the remaining grid area. Finally, Cs are distributed to subcells using a special procedure (see "stochastic" cloud radiative forcing below). Separate radiation calculations are performed for each subcell with clouds, whereas clear sky radiative fluxes are computed only once and used for all subcells. The grid mean radiative heating/cooling distributions are the areal averages over all subcells. This framework can treat both the cloud macrogrouping and the inhomogeneity more rigorously.

As shown in Liang and Wang (1997), when compared with the random overlap treatment, the mosaic treatment that incorporates the "macrogrouping" effect calculates a significantly different atmospheric radiative heating/cooling distribution. In the tropics, it yields a heating in the upper troposphere and a cooling in the lower troposphere, especially near the surface; opposite changes are calculated in the middle-to-high latitudes. Differences in climate response are substantial, where the mosaic treatment corrects several major model biases. For example, the middle-to-upper troposphere of the tropics and subtropics is more than 3° C throughout the year, while the polar night stratosphere in the Northern Hemisphere becomes much warmer, up to 15° C. The study results clearly suggest that the subgrid scale cloud-radiation variability associated with cloud geometric association has an important impact on climate simulation.

"Stochastic" Cloud Radiative Forcing

Perhaps the most interesting aspect of the mosaic approach is the "stochastic" cloud radiative forcing Liang and Wang (1997) implemented to treat the Cs clouds. The stochastic treatment results from special consideration for this cloud type: adjacent layers that contain Cs are vertically aligned by an identical set of random-order subcells to acquire a maximum overlap, whereas discrete Cs layers use an independent set (i.e., generated randomly each time) to treat the overlap, thus producing the "stochastic" characteristics in the cloud radiative forcing.

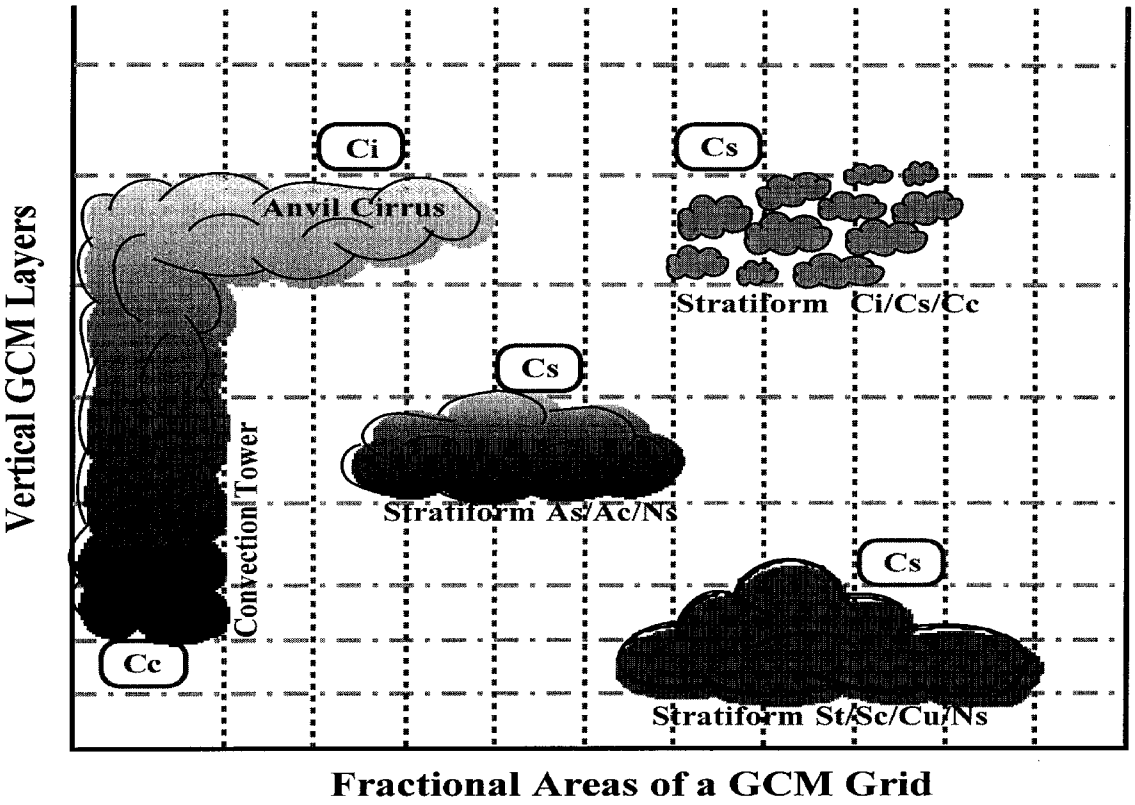

Figure 1. The "mosaic" approach, in which the GCM grid is aggregated into N subcells horizontally so that the vertical association due to increased resolution can be considered more realistically. The GCM predicts individually the fractional coverage of convective (Cc), anvil cirrus (Ci), and stratiform (Cs) clouds, which are therefore subgrid-scale.

Radiative forcing in the "mosaic" approach with its inherent "stochastic" characteristics could differ substantially from those that use random overlap for treating vertical cloud overlap in CCM3 (Kiehl et al. 1996). For example, as illustrated in Figure 2, the mosaic approach tends to calculate a smaller solar radiation input (up to 35 Wm^{-2}) to the model climate system (decreases in TOA forcing), with most of the decreases caused by decreases in the surface forcing (SFC). However, it is particularly interesting to note that the atmospheric absorption becomes larger (up to 10 Wm^{-2}) for the two cases of high-middle clouds and low-middle clouds in the mosaic treatment, as reflected in the steeper slopes in the TOA-SFC plots, but not for the case of high-low clouds. The increased atmospheric absorption is caused by the enhanced water vapor absorption that results from multiple reflections between the clouds.

Cloud Cover Probability Distribution Function

One critical assumption used in Liang and Wang (1997) is that binary clouds (i.e., completely overcast or clear skies) are used in the individual subcells. This simplification is based on the statistics that the probability of either completely overcast or clear skies increases as the observation area decreases.

Liang and Wang (1997) used satellite-measured total cloud cover with data cells of $(50\ km)^2$ over the SGP during the April 6-30, 1994, IOP to examine the cloud cover probability distribution function (PDF) for specified ranges of cloud mean (CM) amount over a grid of $(1000\ km)^2$ area. The results suggest the dominance of either completely overcast or clear skies in the mesoscale cells for all CM values while the fraction of partial cloudy conditions is

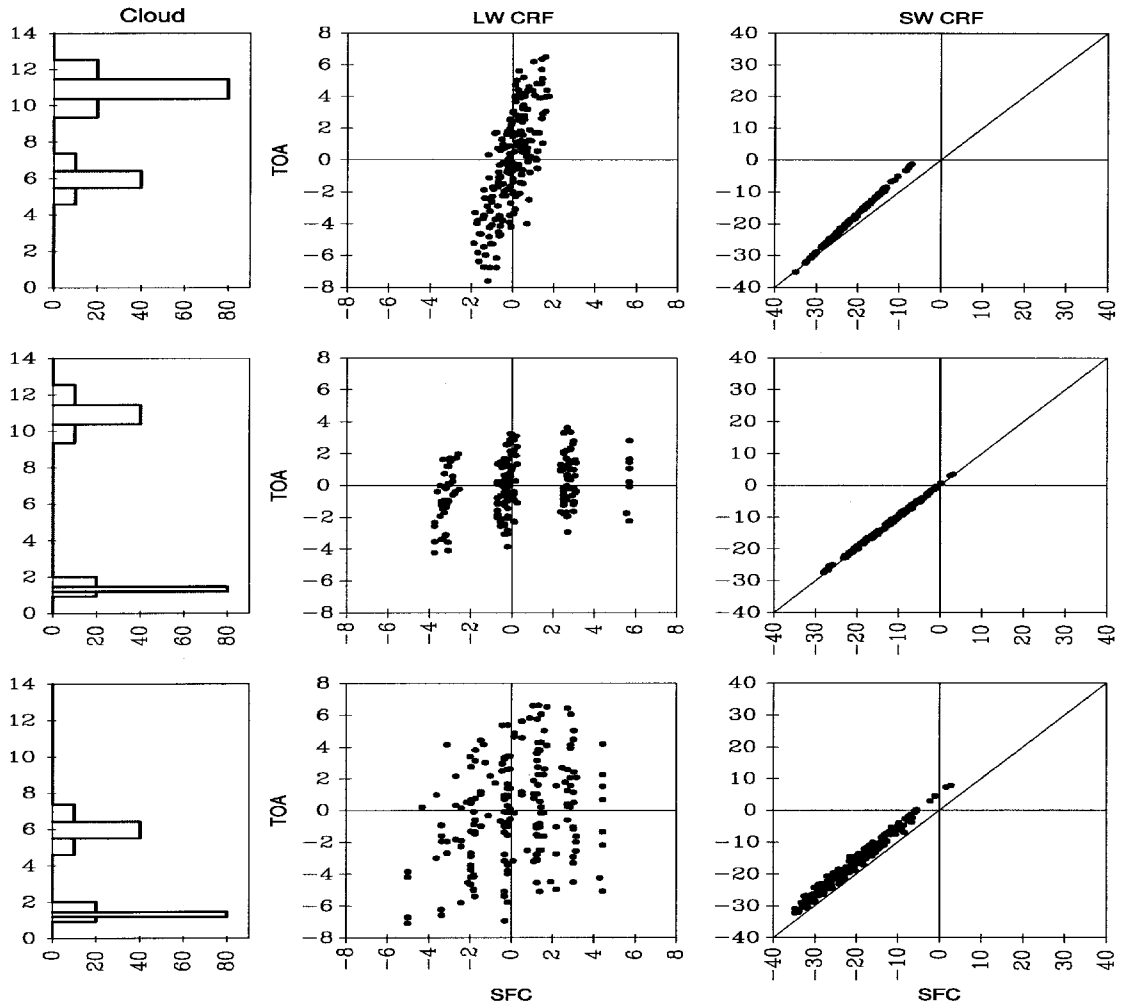

Figure 2. The "stochastic" cloud radiative effects associated with the "mosaic" approach. The longwave (LW) and shortwave (SW) cloud radiative forcing (CRF; Wm^{-2}) at the top-of-atmosphere (TOA) and on the surface (SFC) are the differences between the "mosaic" approach and the CCM3 "random overlap" scheme (Kiehl et al. 1996) for the specified vertical cloud distribution (left panel). Each dot represents one of the 200 mosaic calculations using the McClatchey et al. (1972) mid-latitude summer model atmosphere.

quite small. They found that the PDF changes gradually with CM and that PDFs are symmetric about CM=50%. They further found that the PDFs for high, middle and low clouds are essentially similar to those for total cloud cover. In practical applications, given PDFs, the distribution of subcell cloud fractions can be determined based on GCM-predicted CM values. Because of the variability of cloud overlap and the uncertainties of other cloud information, comparisons of cloud PDFs make the model evaluation more vigorous. Therefore, further analyses of observations and regional model simulations are warranted to examine the PDFs at different climate zones.

Vertical Distribution of Cloud Liquid/ice Water

Because cloud cover is related to the GCM cloud liquid water/ice parameterization, Liang and Wang's (1997) findings were sensitive to the cloud liquid water/ice vertical distribution. In that study, the model, following Kiehl et al. (1996), assumes that liquid water/ice decreases exponentially with altitude where the scale height is a function of latitude. (Note that the distribution is prescribed in diagnostic approach versus calculated in a prognostic approach; see Slingo 1987.) Therefore, the fundamental issue was to determine the degree to which the geographical and vertical distributions of cloud liquid/ice water were

realistic. To make an initial evaluation, we used two types of data: the measurements at the Central Facility/SGP and simulations from a cloud resolving model (CRM) developed at MMM/NCAR.

For the SGP data, we used the measurements of cloud base heights from micropulse lidar (MPL) and column water vapor and cloud liquid/ice paths from microwave radiometer (MWR). Figure 3 shows the summer and winter frequency of cloud occurrence as a function of liquid water path and cloud base height. Clearly, the distribution function exhibits "stochastic" characteristics with strong seasonal variation. During winter, there are more clouds with lower bases and larger liquid water, while during summer the cloud base, with a peak at 4 km, extends to far higher levels. We have also studied cloud frequency as a function of water vapor path and liquid water path (not shown). Again, the seasonal contrast is large: summer clouds with smaller liquid water are usually associated with more water vapor, while the winter statistics have quite different characteristics. In collaboration with L. Harrison and Q. Min (State University of New York at Albany), we are also examining the measurements of surface shortwave fluxes from a multi-filter rotating shadowband radiometer (MFRSR) and cloud optical properties and droplet effective radius derived from MWR and MFRSR, so that the consistency of the statistics between the clouds and shortwave radiation fluxes can be evaluated.

For CRM data, we adopted the results of Wu et al. (1997), who used a 2-D model to simulate a tropical cloud system for a 39-day period (December 5, 1992-January 12, 1993) during the Tropical Ocean Global Atmosphere (TOGA) Coupled Ocean Atmosphere Response Experiment (COARE). The dataset has 3-km horizontal resolution covering the TOGA/COARE 900-km domain. Averaging over the whole domain, the statistics indicate that clouds occur 54% of the time in single (penetrative) towers, 12% in two distinct cells, and 4% in multiple levels.

As shown in Figure 4, most of the penetrative clouds have a peak water content at 6 km, where ice formation is maximized near local temperature -10° C, and a secondary peak at 4.5 km, where liquid growth reaches the maximum above the updraft mass flux maxima. Note that the peak concentration of cloud water is independent of cloud base height, which is different from the exponential decaying vertical profile adopted by CCM3 (Kiehl et al. 1996).

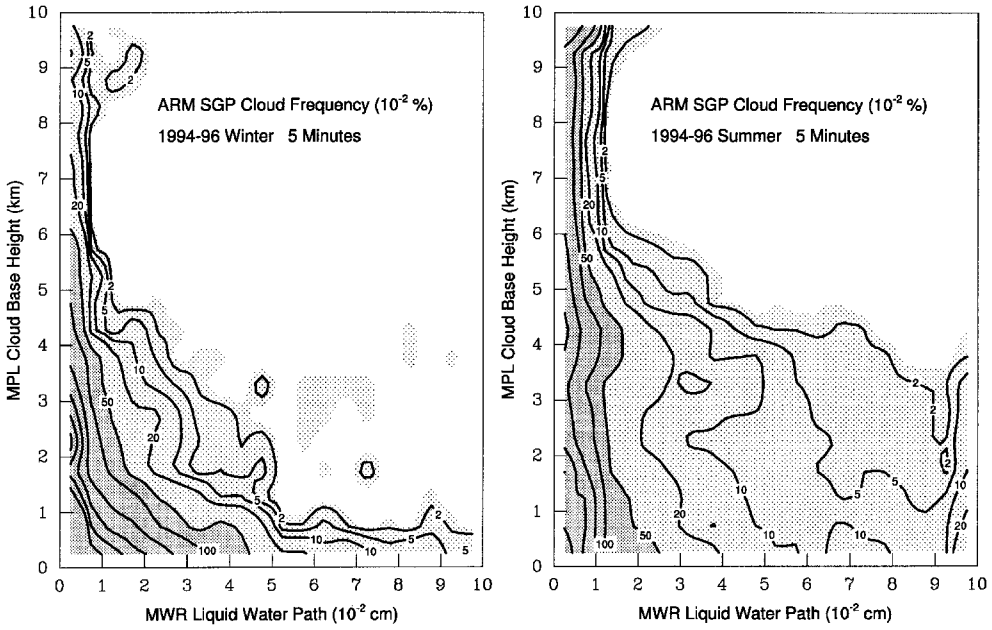

Figure 3. Frequency (in 10-4 unit) of cloud as a function of cloud base height and column liquid water path for winter (December-January-February; left panel) and summer (June-July-August; right panel). The height and path were measured, respectively, by the micropulse lidar (MPL) and microwave radiometer (MWR) at the ARM SGP Central Facility during January 1994 - December 1996. All data are averaged over 5 minutes with contours at 2, 5, 10, 20, 50, 100, 200, 300, 400, and 500 units.

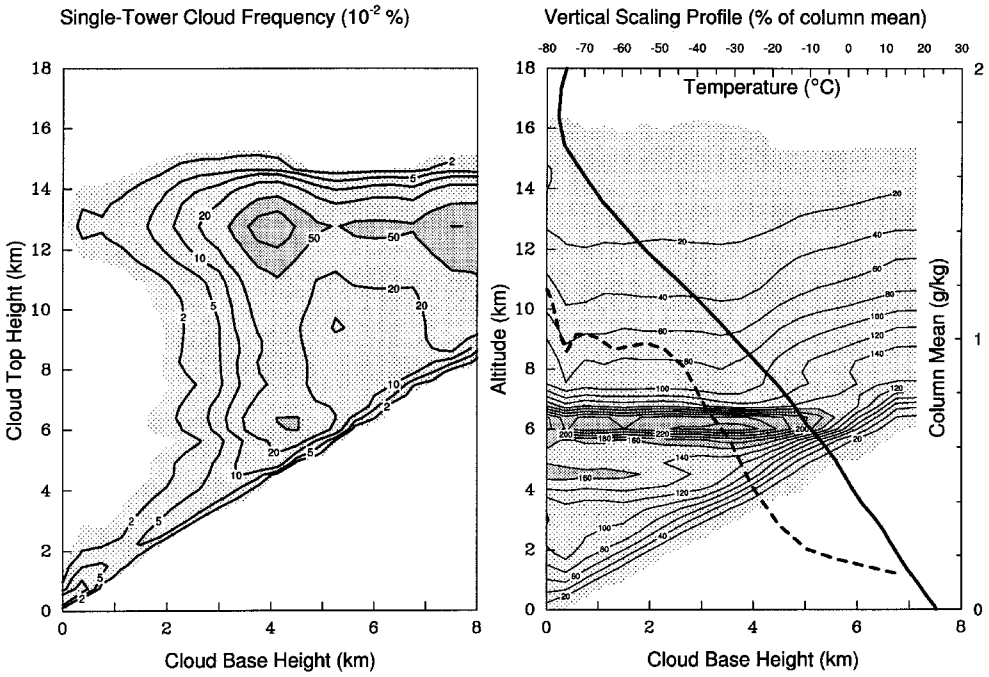

Figure 4. Statistics of a single-tower cloud simulated by the cloud resolving model over TOGA/COARE during 5 December 1992 - 12 January 1993 (Wu et al. 1997). All 15-minute cloud data with 3-km horizontal resolution over a 900-km span are used to identify the statistics of single-tower, which is defined to be an unbroken cloud segment in the vertical. (Left panel) The cloud frequency (in 10^{-4} unit) as a function of cloud base and top heights with contours at 2, 5, 10, 20, 50, and 100 units. (Right panel) The cloud liquid water/ice vertical scaling profile (contours at 20 units) is defined as percentages of the column mean values (dashed line; using the lower and right scales). The domain mean temperature profile (thick solid, using the top and left scales) is also shown.

We have conducted a sensitivity study on the effect of cloud liquid/ice vertical distribution on radiative heating/cooling in the atmosphere. The calculations, shown in Figure 5, are based on an atmospheric model consisting of a 50% clear region and a 50% single cloud tower with two different cloud water profiles (one from CCM3 with exponential decay characteristics and the other derived from the CRM simulations) with identical column amount. It is quite clear that the vertical distribution of cloud water substantially affects the solar and longwave radiative heating/cooling distribution. The most significant difference is the shift of the peak net radiative cooling rate from 2.5° C at 7 km in the exponential profile to 1.5° C at 10 km in the CRM profile.

Radiative Effects of Cirrus Clouds

Parameterizations for the shortwave and longwave radiative effects of cirrus clouds for use in GCMs were developed. In the parameterizations, cloud particles are assumed to be composed of randomly oriented hexagonal crystals. For shortwave radiation, the broad band transmittance, reflectance, and absorptance are expressed as a function of single scattering albedo, asymmetry factor, and optical depth, which in turn are functions of effective particle radius. For longwave radiation, the optical depth and emissivity are expressed in terms of cloud ice water

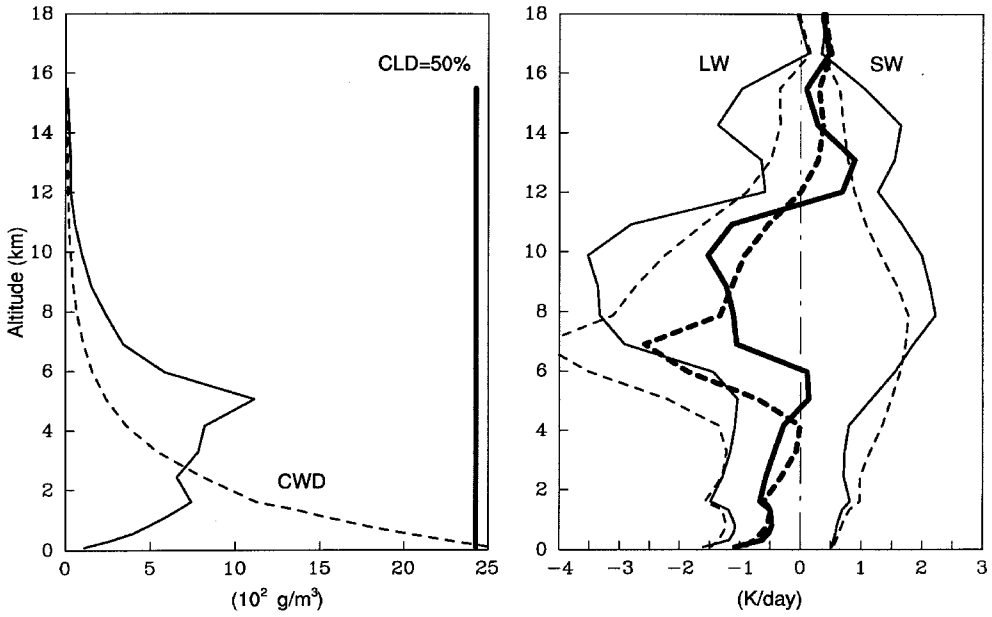

Figure 5. The effect of specified vertical cloud liquid water profiles on the radiative heating/cooling distribution. (Left panel) An atmosphere with 50% clear region and a 50% single cloud tower extending from surface to 15.5 km is used. Two liquid water profiles, an exponential profile from CCM3 (dashed line) and the other from CRM simulation (thin solid line; Figure 4) with identical column water of 0.551 cm. (Right panel) the shortwave and longwave radiative heating rates are calculated based on the McClatchey et al. (1972) tropical model atmospheric temperature and moisture with April 1 solar zenith angle and surface albedo 0.1. Thick solid line is the net (LW+SW) radiative heating.

path. Both the effective particle radius and ice water path are parameterized to be a function of cloud temperature. Details of the new parameterization are described in Joseph and Wang (1995).

Using this new parameterization with satellite-derived high level clouds during the April 1994 IOP over SGP, we conducted a model-to-observation comparison of the downward flux at the surface and outgoing flux at the TOA for both shortwave and longwave radiation. The results suggest that the new parameterization with interactive microphysics and optical properties simulates better agreement with observations. For example, when compared with the old parameterization, the new parameterization reduces the rms difference in the TOA shortwave radiation flux by 50%.

Comparisons of the cloud optical properties, and shortwave and longwave radiative fluxes from the calculations using the new parameterization and the current cirrus schem used in NCAR GENESIS, as well as with observations were conducted. The results indicate that, while the new parameterization calculates more realistic cirrus cloud optical properties, the biases in the calculated radiative fluxes remain large (Joseph and Wang 1997).

References

Dudek, M. P., X.-Z. Liang, and W.-C. Wang, 1996: A regional climate model study of the scale-dependence of cloud-radiation interactions. *J. Climate*, **9**, 1221-1234.

Joseph, E. and W.-C. Wang, 1995: Incorporation of an improved cirrus cloud parameterization into the NCAR-GENESIS climate model. *Proceedings of the Sixth Symposium on Global Change Studies*, pp. 136-141, January 15-20, 1995, Dallas, Texas. American Meteorological Society, Boston, Massachusetts.

Joseph, E., and W.-C. Wang, 1997: Using ARM data to validate an interactive high cloud radiative parameterization for GCMs. *Proceedings of the Ninth Conference on Atmospheric Radiation*, Long Beach, California, February 2-7, 1997. American Meteorological Society, Boston, Massachusetts.

Kiehl, J. T., J. J. Hack, G. B. Bonan, B. A. Boville, B. P. Briegleb, D. L. Williamson, and P. J. Rasch, 1996: Description of the NCAR Community Climate Model (CCM3). NCAR/TN-420+STR. National Center for Atmospheric Research, Boulder, Colorado.

Liang, X.-Z., and W.-C. Wang, 1997: Cloud overlap effects on GCM simulations. *J. Geophys. Res*. (accepted for publication).

McClatchey, R. A., R. W. Fenn, J.E.A. Selby, F. E. Volz, and J. S. Garing, 1972: Optical properties of the atmosphere. AFCRL-72-0497, Air Force Cambridge Research Laboratories, Bedford, Massachusetts.

Slingo, J., 1987: The development and verification of a cloud prediction scheme for the ECMWF model. *Quart. J. Roy. Meteor. Soc*., **113**, 899-927.

Wu, X., W. W. Grabowski, and M. W. Moncrieff, 1997: Long-term evolution of cloud systems in TOGA COARE and their interactions with radiative and surface processes. Part I: Two-dimensional cloud-resolving model. *J. Atmos. Sci*. (accepted for publication).